HHS Public Access

Author manuscript

Science. Author manuscript; available in PMC 2018 July 28.

Published in final edited form as:

Science. 2017 July 28; 357(6349): 400–404. doi:10.1126/science.aan3721.

Control of Species-Dependent Cortico-motoneuronal Connections Underlying Manual Dexterity

Zirong Gu[1], **John Kalamboglas**[2,3], **Shin Yoshioka**[1], **Wenqi Han**[4], **Zhuo Li**[4], **Yuka Imamura Kawasawa**[4,5], **Sirisha Pochareddy**[4], **Zhen Li**[4], **Fuchen Liu**[4], **Xuming Xu**[4], **Sagara Wijeratne**[6], **Masaki Ueno**[1,9], **Emily Blatz**[1], **Joseph Salomone**[1], **Atsushi Kumanogoh**[7], **Mladen-Roko Rasin**[6], **Brian Gebelein**[1], **Matthew T. Weirauch**[8], **Nenad Sestan**[4], **John H. Martin**[*,2,3], and **Yutaka Yoshida**[*,1]

[1]Division of Developmental Biology, Cincinnati Children's Hospital Medical Center, Cincinnati, OH, USA

[2]Department of Physiology, Pharmacology and Neuroscience, City College of the City University of New York, New York, New York, USA

[3]Graduate Center, City University of New York, New York, New York 10017, USA

[4]Department of Neuroscience, Kavli Institute for Neuroscience, Yale School of Medicine, New Haven, CT, USA

[5]Institute for Personalized Medicine, Departments of Biochemistry and Molecular Biology and Pharmacology, Penn State College of Medicine, Pennsylvania 17033, USA

[6]Department of Neuroscience and Cell Biology, Rutgers-RWJ Medical School, Piscatway, NJ, USA

[7]Department of Respiratory Medicine, Allergy and Rheumatic Diseases, Graduate School of Medicine, Osaka University, Suita, Japan

[8]Center for Autoimmune Genomics and Etiology, Division of Biomedical Informatics, and Division of Developmental Biology, Cincinnati Children's Hospital Medical Center, Cincinnati, OH, USA

[9]Precursory Research for Embryonic Science and Technology (PRESTO), Japan Science and Technology Agency (JST), Kawaguchi, Saitama, 332-0012, Japan

Abstract

Superior manual dexterity in higher primates emerged together with the appearance of cortico-motoneuronal (CM) connections during the evolution of the mammalian corticospinal (CS) system. Previously thought to be unique to higher primates, we identified transient CM connections in early postnatal mice, which are eventually eliminated by Sema6D-PlexA1 signaling. *PlexA1* mutant mice maintain CM connections into adulthood and exhibit superior manual dexterity compared to controls. Finally, differing *PlexA1* expression in layer 5 of the motor cortex, which is strong in wild-type mice but weak in humans, may be explained by FEZF2-mediated *cis*-regulatory elements that are found only in higher primates. Thus, species-dependent

[*]Corresponding author. Yutaka.Yoshida@cchmc.org or jmartin@ccny.cuny.edu.

regulation of *PlexA1* expression may have been crucial in the evolution of mammalian CS systems that improved fine motor control in higher primates.

The emergence of sophisticated motor and cognitive abilities in humans has been accompanied by complex CNS specializations. Axon trajectory and connectivity modifications contributed to an advanced brain that enabled higher cognitive functions and finer motor control (1). Species differences in axonal trajectories, circuit connectivity, and function, are exemplified by the CS tract (CST), which is essential for voluntary movement. A key feature distinguishing the CS systems of higher primates is hand dexterity control. This dexterity likely arises from the unique monosynaptic connections between CS neurons and motor neurons (MNs) that control hand muscles in higher primates (2). In other mammals, these cortico-motoneuronal (CM) connections may fail to develop, or they may form and then become actively eliminated. CS circuit pathways also differ substantially, with CSTs in higher primates descending within the ventral and lateral funiculi of the spinal cord, and those in rodents descending in the dorsal funiculus (2).

There are neither significant contacts between CST axons and MNs, nor functional CM connections in adult rodents (3–6). To examine early postnatal mice for CM connections, we performed monosynaptic rabies virus tracing from forelimb muscles at postnatal day 3 (P3) (Fig. 1A). When motor cortices were analyzed for mCherry expression 8 days post injection (dpi), we observed mCherry^{+} CS neurons in both hemispheres with more extensive contralateral labeling (Figs. 1B and 1D), providing evidence of CM connections in juvenile mice.

We then labeled CST fibers genetically using *Emx1-Cre; cc-GFP* mice and examined the postnatal CST innervation patterns within the spinal cord (fig. S1A and S1C–S1M). In P2 mice, eGFP^{+} CST axons were detected in the ventral-most region of the dorsal funiculus (dCST) at upper cervical levels only (figs. S1C–S1E). We also observed eGFP^{+} CST fibers in the ventral and lateral funiculi (vCST and lCST; together vlCST) at cervical, thoracic, and lumbar levels at P2 (figs. S1C–S1K, and purple bars in S1N). The density of the eGFP^{+} vlCST decreased at P10 and was undetectable at P14 and beyond (figs. S1B, and S1L–S1N). Unilateral injections of *AAV1-hSyn-Cre* into the motor cortex of *ccGFP* mice at P4 led to vlCST labeling in the ipsilateral spinal cord at P10 (figs. S2A–S2F). The vlCST constituted about 20% of all the descending CSTs (figs. S2G–S2J). Analysis of the cervical spinal cords of P2 or P7 mice showed that presynaptic terminals of the ipsilateral vlCST or contralateral dCST form contacts on MNs (figs. S2K–S2L).

Next, we examined whether the semaphorin (Sema) family of repulsive molecules, and their receptors (plexins (Plexs) and neuropilins (Npns)) are involved in axon pruning of the vlCST and the elimination of CM connections (figs. S3A–S3E). Targeted deletions revealed that only *PlexA1*$^{fl/fl}$*; Emx1-Cre* and *Sema6D*$^{-/-}$ mice retained CST axons in the ventral and lateral funiculi until P38 (Figs. 1E–1P and figs. S3F–S3M). Both Sema6C and Sema6D are PlexA1 ligands, however, only mice lacking Sema6D exhibited persistent vlCSTs (Figs. 1M–1P and figs. S3L–S3M). No obvious defects were found in CST trajectories around the decussation region of *PlexA1* and *Sema6D* mutant mice (fig. S4).

The PlexA1 receptor and *Sema6D* were expressed in CS axons in the brain (fig. S5) and in the ventral spinal cord and white matter, respectively, with *Sema6D* expression relatively restricted to P6 mice (figs. S6E–S6J). CS circuit labeling using dual-color retrograde virus tracing demonstrated that the dCST and vlCST in adult *PlexA1$^{fl/fl}$; Emx1-Cre* mice were derived from the same CS neurons (fig. S7).

Anterograde tracing in adult mice revealed more numerous contacts between the CST and MNs in *PlexA1$^{fl/fl}$; Emx1-Cre* mice compared to controls (fig. S8) without any obvious defects in projection patterns to brainstem motor pathways (fig. S9), consistent with *Sema6D* expression being restricted to the spinal cord and absent from those brain regions (figs. S6A–S6D). A dorsal hemisection lesion at the C3/4 spinal level in adult mice followed by removal of the dCST below the lesion site (fig. S10A) revealed that individual vlCST axons produced multiple collaterals, some of which crossed the midline, exhibiting arborization patterns that were similar to those described in adult rhesus monkey CSTs (figs. S10) (7, 8). Monosynaptic rabies virus assays revealed a significant increase in CM connections in early postnatal *PlexA1* mutant mice compared to same-age controls (Figs. 1A–1D), with no changes in monosynaptic connections between MNs and premotor interneurons (INs), or other descending brainstem nuclei (figs. S11–S13).

As monosynaptic rabies virus tracing from muscles is ineffective after P10 (9), we performed electrophysiology to determine whether functional CM connections are maintained in adult *PlexA1$^{fl/fl}$; Emx1-Cre* mice. We used stimulus triggered averaging (StTA) to detect the latency of post-stimulus facilitation (PStF) of EMGs recorded from forelimb muscles in response to motor cortex stimulation (10). *PlexA1$^{fl/fl}$; Emx1-Cre* mice displayed shorter PStF latencies for both contralateral and ipsilateral CS circuits (Figs. 2A–2G and fig. S14) with no obvious changes in the currents required to evoke PStF or the thresholds for conventional intracortical microstimulation (ICMS; figs. S15, A and B). We compared the PStF latencies from forelimb muscles following CST axon stimulation in the ventral portion of the C5 dorsal column (DC) (Fig. 2H). Antidromic field recordings from the motor cortex confirmed CST activation in our stimulation paradigm from this ventral stimulation site, but not from the dorsal portion of the DC where ascending sensory fibers reside (Figs. 2I–2J, and fig. S16). PStF latencies evoked by ventral DC stimulation (CST) in *PlexA1$^{fl/fl}$; Emx1-Cre* mice were significantly shorter than those observed in *PlexA1$^{fl/fl}$* mice (Figs. 2K–2N), whereas stimulation of the dorsal DC showed no differences in evoked EMG responses between *PlexA1$^{fl/fl}$; Emx1-Cre* and control mice (fig. S17). Furthermore, we found that current amplitudes used to evoke EMG responses through either the dorsal DC (afferent fibers) or the ventral DC (CST) were similar between control and *PlexA1$^{fl/fl}$; Emx1-Cre* mice (figs. S15, C and D).

CM connections are critical for fine manual dexterity in primates (11, 12). Rodents show a limited degree of manual dexterity without CM connections by using coordinated paw movements to manipulate food pieces (13). To measure manual dexterity, we performed the capellini handling test (Fig. 3A, and figs. S18E–S18G) with mice that had received *AAV1-Cre* bilateral motor cortex injections at P2 (*PlexA1$^{fl/fl}$; AAV1-Cre* mice), which produces similar developmental pruning defects as those observed in the *Emx1-Cre*-mediated mutants (figs. S18A–S18D). *PlexA1$^{fl/fl}$; AAV1-Cre* mice ate significantly faster than *PlexA1$^{fl/+}$;*

AAV1-Cre mice on all testing days (Fig. 3B, fig. S18H, Movies S1–S4), and exhibited significantly higher paw adjustment rates on all four testing days compared to *PlexA1*$^{fl/+}$*; AAV1-Cre* mice (Fig. 3C and fig. S18I). In addition, *PlexA1*$^{fl/fl}$*; AAV1-Cre* mice displayed fewer atypical handling patterns than *PlexA1*$^{fl/+}$*; AAV1-Cre* mice (Fig. 3D, and figs. 18J–18Q). *PlexA1*$^{fl/fl}$*; Emx1-Cre* mice also outperformed control mice during a sticky tape removal test (figs. S19, A and B).

To evaluate grasping, we designed and implemented a new prehension test (fig. S20) where animals had to use their paws to reach, grasp and retrieve a food pellet (Figs. 3E–3G). *PlexA1*$^{fl/fl}$*; AAV1-Cre* mice exhibited significantly higher grasping success rates than controls (*PlexA1*$^{fl/+}$*; AAV1-Cre* and *PlexA1*$^{fl/fl}$*; AAV1-td*), while pellet consumption time was indistinguishable between the two groups (Figs. 3H–3K, Movies S5 and S6). We also found no obvious deficits in grip strength (fig. S19C) or grid-walking in *PlexA1*$^{fl/fl}$*; Emx1-Cre* mice (fig. S19D). Behavioral changes were not associated with any obvious changes in cortico-cortical projections, laminar ation, or dendritic development (by Golgi analysis) of CS neurons in *PlexA1*$^{fl/fl}$*; Emx1-Cre* mice (fig. S21).

The presence of CM connections and the vlCST in adult *PlexA1* mutant mice bear a remarkable resemblance to human CS circuits, prompting us to examine *PLEXA1* expression within the developing human motor cortex. Human mid-fetal cortices at 20 post-conception *weeks* (pcw), which corresponds to the early postnatal mouse cortex, showed very weak *PLEXA1* expression in layer 5 CS neurons, but strong expression in layer 6 of the putative motor cortex, which does not give rise to CST projections (Fig. 4A).

To determine whether species-dependent *cis*-regulatory elements might define *PLEXA1* expression levels in layer 5, we first identified and compared putative orthologous enhancer regions between humans and mice. Enhancers were identified based on features indicative of active regulatory regions, including H3K4me3 and H3K27ac histone marks, DNase hypersensitivity, and DNA conservation across mammals. This resulted in a ~5 kilobase putative orthologous enhancer in humans and mice (fig. S22). Within the putative human enhancer, we identified a total of 28 putative FEZF2 binding sites. FEZF2 (also known as FEZL and ZFP312), encoding a zinc-finger transcription repressor (14) required for CS tract development (15), was expressed in the putative layer 5 of the 22 pcw human brain (fig. S26A). Three FEZF2 binding sites correspond to the typical “CTNCANCN” Fezf2 binding site (figs. S23–S25, blue bars) (16), with the remaining 25 resembling a recently described “CGCCGC” element (figs. S23–S25, green and red bars) (17). 5 of the total 28 sites were conserved in both humans and mice (fig. S24, green bars), while 23 of them were only found in humans, resulting in a putative homotypic cluster of 23 human FEZF2 binding sites (Fig. 4B, figs. S22A, S23–S25) (18, 19). Humans, chimpanzees, gorillas, orangutans, and baboons, which all have CM connections (2), all possess these FEZF2 binding sites in their putative *PlexA1 cis*-regulatory elements (Fig. 4B, and figs. S23–S25). In contrast, mice, rats, and rabbits, as well as some primates, such as marmosets and bushbabies that lack CM connections (2), either lack these FEZF2 binding sites completely or have nucleotide mismatches that are predicted to decrease FEZF2 binding (Fig. 4B, figs. S23–S25). Electrophoretic mobility shift assays (EMSAs) demonstrated binding of FEZF2 to the human FEZF2 binding site, but weaker binding to the homologous mouse sequence and

human sequence with point mutations (making it identical to the mouse sequence) (fig. S26B).

Using *in vitro* luciferase assays, we found that FEZF2 represses the transcriptional activity of the human, but not mouse, *cis*-regulatory elements (Fig. 4C, figs. S26, C and D). Constructs with point mutations in both FEZF2 motifs showed a complete loss in FEZF2-mediated repression (Fig. 4C). Enhancer analysis by transfecting constructs with the FEZF2 *cis*-regulatory elements to primary cortical neuron cultures from wild-type and *Fezf2* mutant mice demonstrated a strong FEZF2-mediated repression of the putative human *cis*-regulatory elements in $BCL11B^+$ ($CTIP2^+$) layer 5 cortical neurons (figs. S27 and S28). Further analysis of transgenic mice expressing GFP under the human FEZF2 *cis*-regulatory elements revealed that the putative human *cis*-regulatory elements drove strong expression of GFP in layer 6, but not layer 5, of the motor cortex, recapitulating the *PLEXA1* expression in the human motor cortex (Figs. 4, D and E, and fig. S29). Transgenic mice with the human *FEZF2* binding sites mutated drove robust expression in layer 5 neurons and CS axons (Figs. 4, F and G, and fig. S29). Expression of *PlexA1* was not altered in the cortices of *Fezf2* mutant mice at P0 (figs. S26, E and F).

Considering that CM connections seem beneficial for mice, why are they eliminated? Perhaps increased manual dexterity confers no fitness advantages to quadrupedal animals, or perhaps it even imposes a fitness burden. For example, maintenance of CM connections in mice may disrupt development and function of other spinal motor circuits, such as those for forelimb locomotion rather than manipulation. Another question lies in the preservation of transient CM connections in wild-type mice. Perhaps they play a temporary developmental role in assisting the establishment of other spinal neural circuits. Our findings, providing insight into the specific contributions of CM connections to dexterous manipulations by mice, serve as a stepping stone towards answering these questions, and present a potential mechanism for how CM connections emerged during mammalian evolution.

Supplementary Material

Refer to Web version on PubMed Central for supplementary material.

Acknowledgments

We are grateful to M. Baccei, J. N.Betley, K. Campbell, S. Crone, C. Gu, T. Isa, D. Ladle, M. Nakafuku, S. and R. Yu for critical comments on the manuscript. We thank *Boston Children's Hospital Viral Core* (supported by core grant NEI 5P30EY012196-17) for making the AAV6-G virus. We thank P. Arlotta for the Fezf2 construct. Z.G. and E.B. were supported by the Graduate Summer Undergraduate Mentoring Program at the University of Cincinnati. MTW is supported by the National Institutes of Health (NIH) grants R01 NS099068 and R21 HG008186, Lupus Research Alliance "Novel Approaches" award, and a CCHMC CpG Pilot Study award. N.S. is supported by NIH grants MH106934 and MH103339. J.H.M. and Y.Y. are supported by NIH grants NS079569 and NS093002, respectively. All data are available in the main texts and supplementary information. Z.G. and Y.Y. conceived of the project and contributed to experimental design and interpretation. Z.G. performed most of the experiments. Z.G., J.K. and J.H.M. designed the cortico-muscular electrophysiology assay, performed EMG recordings, and analyzed and interpreted the electrophysiological data. Y.I.K., W.H., Z.L., Z.L., F.L., S.P., X.X., and N.S. performed the *in situ* hybridizations using human tissues, ChIP-seq using human and mouse tissues, and culture experiments using *Fezf2-floxed* mice. S.Y. contributed to cloning of the human and mouse genomic regions and the luciferase assays. E.B. performed the grid-walking test and contributed to the immunochemistry studies. M.U. purified rabies viruses and assisted in the dorsal hemisection surgery. S.W. and M.R. analyzed the cortical layers and cortico-cortical projections, and also conducted the Golgi analyses. J.S. and B.G. performed the EMSA analyses. M.T.W. performed the cross-species *cis*-regulatory element comparisons. A.K. provided the *Sema6D* mutant mice. Y.Y.

supervised all aspects of the work, and Z.G. J.H.M, and Y.Y. prepared the manuscript with contributions from other authors.

REFERENCES AND NOTES

1. Krubitzer L. The magnificent compromise: cortical field evolution in mammals. Neuron. 2007; 56:201–208. [PubMed: 17964240]
2. Lemon RN. Descending pathways in motor control. Annu Rev Neurosci. 2008; 31:195–218. [PubMed: 18558853]
3. Yang HW, Lemon RN. An electron microscopic examination of the corticospinal projection to the cervical spinal cord in the rat: lack of evidence for cortico-motoneuronal synapses. Exp Brain Res. 2003; 149:458–469. [PubMed: 12677326]
4. Alstermark B, Ogawa J. In vivo recordings of bulbospinal excitation in adult mouse forelimb motoneurons. J Neurophysiol. 2004; 92:1958–1962. [PubMed: 15084639]
5. Alstermark B, Ogawa J, Isa T. Lack of monosynaptic corticomotoneuronal EPSPs in rats: disynaptic EPSPs mediated via reticulospinal neurons and polysynaptic EPSPs via segmental interneurons. J Neurophysiol. 2004; 91:1832–1839. [PubMed: 14602838]
6. Jiang YQ, Zaaimi B, Martin JH. Competition with Primary Sensory Afferents Drives Remodeling of Corticospinal Axons in Mature Spinal Motor Circuits. J Neurosci. 2016; 36:193–203. [PubMed: 26740661]
7. Rosenzweig ES, et al. Extensive spontaneous plasticity of corticospinal projections after primate spinal cord injury. Nat Neurosci. 2010; 13:1505–1510. [PubMed: 21076427]
8. Park MC, Belhaj-Saif A, Cheney PD. Properties of primary motor cortex output to forelimb muscles in rhesus macaques. J Neurophysiol. 2004; 92:2968–2984. [PubMed: 15163675]
9. Stepien AE, Tripodi M, Arber S. Monosynaptic rabies virus reveals premotor network organization and synaptic specificity of cholinergic partition cells. Neuron. 2010; 68:456–472. [PubMed: 21040847]
10. Fetz EE, Cheney PD, German DC. Corticomotoneuronal connections of precentral cells detected by postspike averages of EMG activity in behaving monkeys. Brain Res. 1976; 114:505–510. [PubMed: 821592]
11. Heffner R, Masterton B. Variation in form of the pyramidal tract and its relationship to digital dexterity. Brain Behav Evol. 1975; 12:161–200. [PubMed: 1212616]
12. Lawrence DG, Hopkins DA. The development of motor control in the rhesus monkey: evidence concerning the role of corticomotoneuronal connections. Brain. 1976; 99:235–254. [PubMed: 825185]
13. Allred RP, et al. The vermicelli handling test: a simple quantitative measure of dexterous forepaw function in rats. J Neurosci Methods. 2008; 170:229–244. [PubMed: 18325597]
14. Shimizu T, et al. Zinc finger genes Fezf1 and Fezf2 control neuronal differentiation by repressing Hes5 expression in the forebrain. Development. 2010; 137:1875–1885. [PubMed: 20431123]
15. Shibata M, Gulden FO, Sestan N. From trans to cis: transcriptional regulatory networks in neocortical development. Trends Genet. 2015; 31:77–87. [PubMed: 25624274]
16. Chen L, Zheng J, Yang N, Li H, Guo S. Genomic selection identifies vertebrate transcription factor Fezf2 binding sites and target genes. J Biol Chem. 2011; 286:18641–18649. [PubMed: 21471212]
17. Lodato S, et al. Gene co-regulation by Fezf2 selects neurotransmitter identity and connectivity of corticospinal neurons. Nat Neurosci. 2014; 17:1046–1054. [PubMed: 24997765]
18. Gotea V, et al. Homotypic clusters of transcription factor binding sites are a key component of human promoters and enhancers. Genome Res. 2010; 20:565–577. [PubMed: 20363979]
19. Ezer D, Zabet NR, Adryan B. Homotypic clusters of transcription factor binding sites: A model system for understanding the physical mechanics of gene expression. Comput Struct Biotechnol J. 2014; 10:63–69. [PubMed: 25349675]
20. Gorski JA, et al. Cortical excitatory neurons and glia, but not GABAergic neurons, are produced in the Emx1-expressing lineage. J Neurosci. 2002; 22:6309–6314. [PubMed: 12151506]

21. Nakamura T, Colbert MC, Robbins J. Neural crest cells retain multipotential characteristics in the developing valves and label the cardiac conduction system. Circ Res. 2006; 98:1547–1554. [PubMed: 16709902]
22. Wichterle H, Lieberam I, Porter JA, Jessell TM. Directed differentiation of embryonic stem cells into motor neurons. Cell. 2002; 110:385–397. [PubMed: 12176325]
23. Gu C, et al. Neuropilin-1 conveys semaphorin and VEGF signaling during neural and cardiovascular development. Dev Cell. 2003; 5:45–57. [PubMed: 12852851]
24. Walz A, Rodriguez I, Mombaerts P. Aberrant sensory innervation of the olfactory bulb in neuropilin-2 mutant mice. J Neurosci. 2002; 22:4025–4035. [PubMed: 12019322]
25. Yoshida Y, Han B, Mendelsohn M, Jessell TM. PlexinA1 signaling directs the segregation of proprioceptive sensory axons in the developing spinal cord. Neuron. 2006; 52:775–788. [PubMed: 17145500]
26. Takamatsu H, et al. Semaphorins guide the entry of dendritic cells into the lymphatics by activating myosin II. Nat Immunol. 2010; 11:594–600. [PubMed: 20512151]
27. Suto F, et al. Plexin-a4 mediates axon-repulsive activities of both secreted and transmembrane semaphorins and plays roles in nerve fiber guidance. J Neurosci. 2005; 25:3628–3637. [PubMed: 15814794]
28. Han W, et al. TBR1 directly represses Fezf2 to control the laminar origin and development of the corticospinal tract. Proc Natl Acad Sci U S A. 2011; 108:3041–3046. [PubMed: 21285371]
29. DeBoer EM, et al. Prenatal deletion of the RNA-binding protein HuD disrupts postnatal cortical circuit maturation and behavior. J Neurosci. 2014; 34:3674–3686. [PubMed: 24599466]
30. Schaeren-Wiemers N, Gerfin-Moser A. A single protocol to detect transcripts of various types and expression levels in neural tissue and cultured cells: in situ hybridization using digoxigenin-labelled cRNA probes. Histochemistry. 1993; 100:431–440. [PubMed: 7512949]
31. Serradj N, et al. EphA4-mediated ipsilateral corticospinal tract misprojections are necessary for bilateral voluntary movements but not bilateral stereotypic locomotion. J Neurosci. 2014; 34:5211–5221. [PubMed: 24719100]
32. Asante CO, Martin JH. Differential joint-specific corticospinal tract projections within the cervical enlargement. PLoS One. 2013; 8:e74454. [PubMed: 24058570]
33. Tennant KA, et al. The vermicelli and capellini handling tests: simple quantitative measures of dexterous forepaw function in rats and mice. J Vis Exp. 2010
34. Starkey ML, et al. Assessing behavioural function following a pyramidotomy lesion of the corticospinal tract in adult mice. Exp Neurol. 2005; 195:524–539. [PubMed: 16051217]
35. Bouet V, et al. The adhesive removal test: a sensitive method to assess sensorimotor deficits in mice. Nat Protoc. 2009; 4:1560–1564. [PubMed: 19798088]
36. Sestan N, Artavanis-Tsakonas S, Rakic P. Contact-dependent inhibition of cortical neurite growth mediated by notch signaling. Science. 1999; 286:741–746. [PubMed: 10531053]
37. Consortium EP. An integrated encyclopedia of DNA elements in the human genome. Nature. 2012; 489:57–74. [PubMed: 22955616]
38. Weirauch MT, Hughes TR. A catalogue of eukaryotic transcription factor types, their evolutionary origin, and species distribution. Subcell Biochem. 2011; 52:25–73. [PubMed: 21557078]
39. Stormo GD. Consensus patterns in DNA. Methods Enzymol. 1990; 183:211–221. [PubMed: 2179676]
40. Uhl JD, Zandvakili A, Gebelein B. A Hox Transcription Factor Collective Binds a Highly Conserved Distal-less cis-Regulatory Module to Generate Robust Transcriptional Outcomes. PLoS Genet. 2016; 12:e1005981. [PubMed: 27058369]
41. Pennacchio LA, et al. In vivo enhancer analysis of human conserved non-coding sequences. Nature. 2006; 444:499–502. [PubMed: 17086198]
42. Uchikawa M, Ishida Y, Takemoto T, Kamachi Y, Kondoh H. Functional analysis of chicken Sox2 enhancers highlights an array of diverse regulatory elements that are conserved in mammals. Dev Cell. 2003; 4:509–519. [PubMed: 12689590]
43. Takemoto T, et al. Tbx6-dependent Sox2 regulation determines neural or mesodermal fate in axial stem cells. Nature. 2011; 470:394–398. [PubMed: 21331042]

44. Koo J, Shim S, Gu C, Yoo O, Park S. Identification of an enhancer region in the mouse ephA8 locus directing expression to the anterior region of the dorsal mesencephalon. Dev Dyn. 2003; 226:596–603. [PubMed: 12666197]

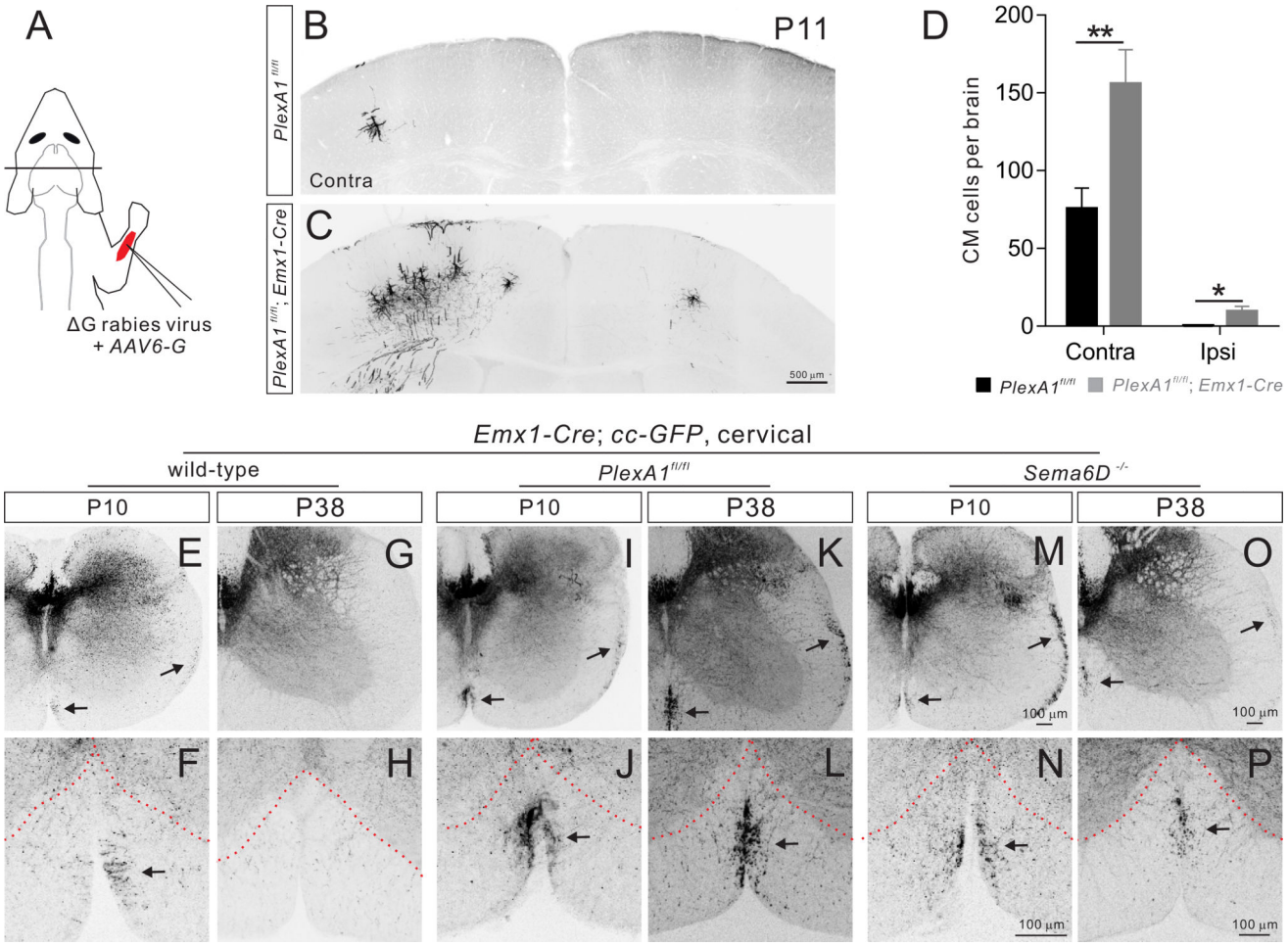

Fig. 1. Elimination of CM connections and the vlCST by Sema6D-PlexA1 signaling in early postnatal mice

(**A**) Experimental scheme for identifying CM connections. Rab-mCherry and *AAV6-G* were co-injected into forelimb muscles of P3 mice. (**B** and **C**) Coronal brain sections from P11 control (*PlexA1*$^{fl/fl}$, n=7; B) and *PlexA1* mutant (*PlexA1*$^{fl/fl}$*; Emx1-Cre*, n=8; C) mice showing labeling of CM cells 8 days after Rab-mCherry virus injections into forelimb muscles. Scale bar, 500 μm. (**D**) Quantification of CM cells. (**E–P**) Cervical spinal cord sections from wild-type (P10, **E** and **F**; P38, **G** and **H**), *PlexA1*$^{fl/fl}$ (P10, **I** and **J**; P38, **K** and **L**), and *Sema6D*$^{-/-}$ (P10, **M** and **N**; P38, **O** and **P**) mice. Scale bars, 100 μm.

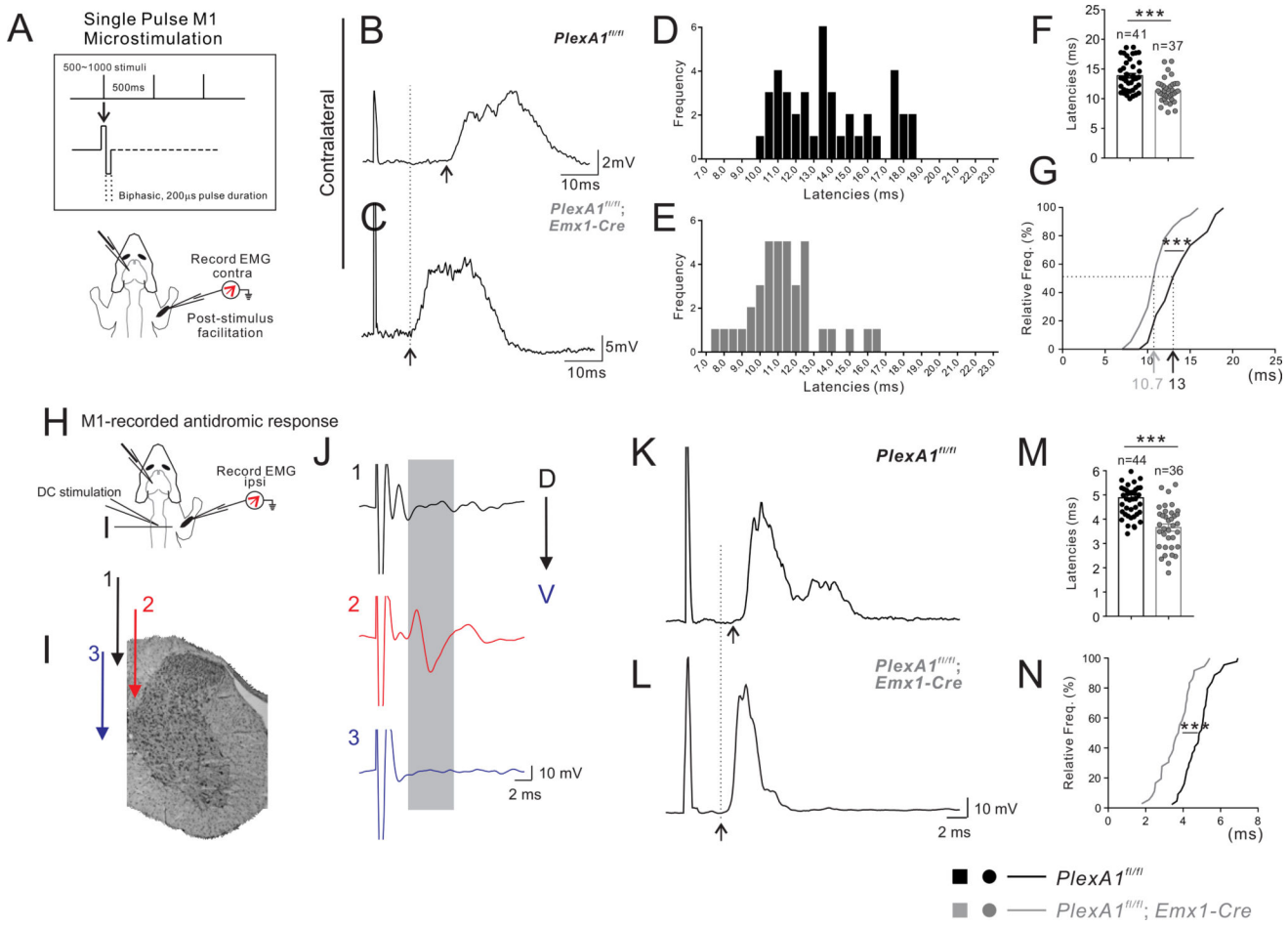

Fig. 2. Functional CM connections in adult *PlexA1$^{fl/fl}$; Emx1-Cre* mice

(**A**) Schematic diagram of experiment to examine PStF in adult mice (3 months or older). EMG recordings from contralateral flexor carpi radialis and biceps brachii muscles. (**B** and **C**) Contralateral PStF from control (B, *PlexA1$^{fl/fl}$*) and mutant (C, *PlexA1$^{fl/fl}$; Emx1-Cre*) mice. (**D** and **E**) Frequency distributions of contralateral PStF values from control (D, *PlexA1$^{fl/fl}$*, n=6; wild-type, n=3) and *PlexA1$^{fl/fl}$; Emx1-Cre* (E, n=8) mice. (**F**) PStF latencies following motor cortex stimulation in *PlexA1$^{fl/fl}$* (41 stimulation sites, median delay=11.34 ms) and *PlexA1$^{fl/fl}$; Emx1-Cre* (37 stimulation sites, median delay=13.88 ms) mice. (**G**) Cumulative frequency distribution histogram. *PlexA1$^{fl/fl}$; Emx1-Cre* (gray line), *PlexA1$^{fl/fl}$* mice (black line). (**H**) Schematic diagram of DC electrical stimulation-evoked muscle PStF. (**I**) Section from a DC stimulation experiment, showing the 3 electrode locations used to evoke M1 antidromic responses. (**J**) Electrical stimulation of the ventral DC evokes an antidromic field potential in the motor cortex. 1: Dorsal DC stimulation, where afferent fibers are located; 2: Ventral DC stimulation (where CST fibers are located); 3: stimulation of the central canal. (**K–L**) PStF traces derived from average EMG responses evoked by ventral DC sites in *PlexA1$^{fl/fl}$* (K) and *PlexA1$^{fl/fl}$; Emx1-Cre* (L) mice. (**M**) PStF latencies in *PlexA1$^{fl/fl}$* (44 sites from 8 animals, median delay=4.88 ms) and *PlexA1$^{fl/fl}$; Emx1-Cre* (36 sites from 6 animals, median delay=3.66 ms) mice. (**N**) Cumulative frequency

distribution plot of PStF latencies from *PlexA1*$^{fl/fl}$*; Emx1-Cre* (gray line), *PlexA1*$^{fl/fl}$ mice (black line). Arrows indicate the onsets of EMG responses (B, C, K, and L).

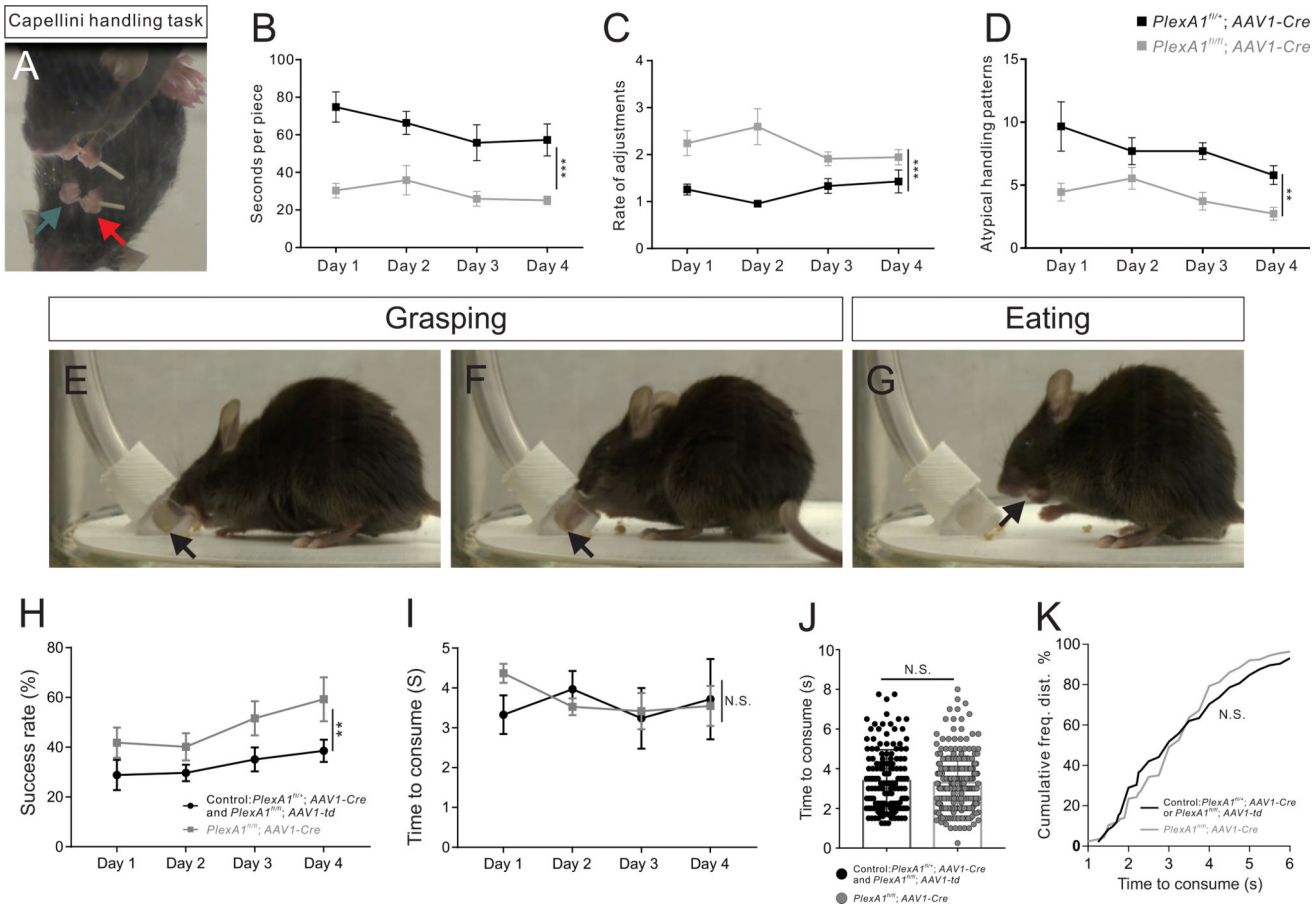

Fig. 3. Adult *PlexA1* mutant mice outperform controls in dexterous manipulation tasks

(**A**) Mouse performing the capellini handling test. Guiding and grasping hands are indicated by green and red arrows, respectively. (**B–D**) Results of the capellini handling test in 2 month-old control (*PlexA1$^{fl/+}$; AAV1-Cre*, n=10) and *PlexA1$^{fl/fl}$; AAV1-Cre* (n=10) mice during 4 testing days. Rate of adjustment = average number of paw adjustments per piece/ eating time. (**E–G**) A mouse during the grasping test. Food pellets are indicated by black arrows. (**H–I**) Grasping success and consumption time in 3 month-old control (*PlexA1$^{fl/+}$; AAV1-Cre*, n=3 and *PlexA1$^{fl/fl}$; AAV1-td*, n=4) and *PlexA1$^{fl/fl}$; AAV1-Cre* (n=8) mice over 4 testing days. (**J–K**) Quantification and frequency distributions of pellet consumption time by control (145 trials) and *PlexA1$^{fl/fl}$; AAV1-Cre* (251 trials) mice.

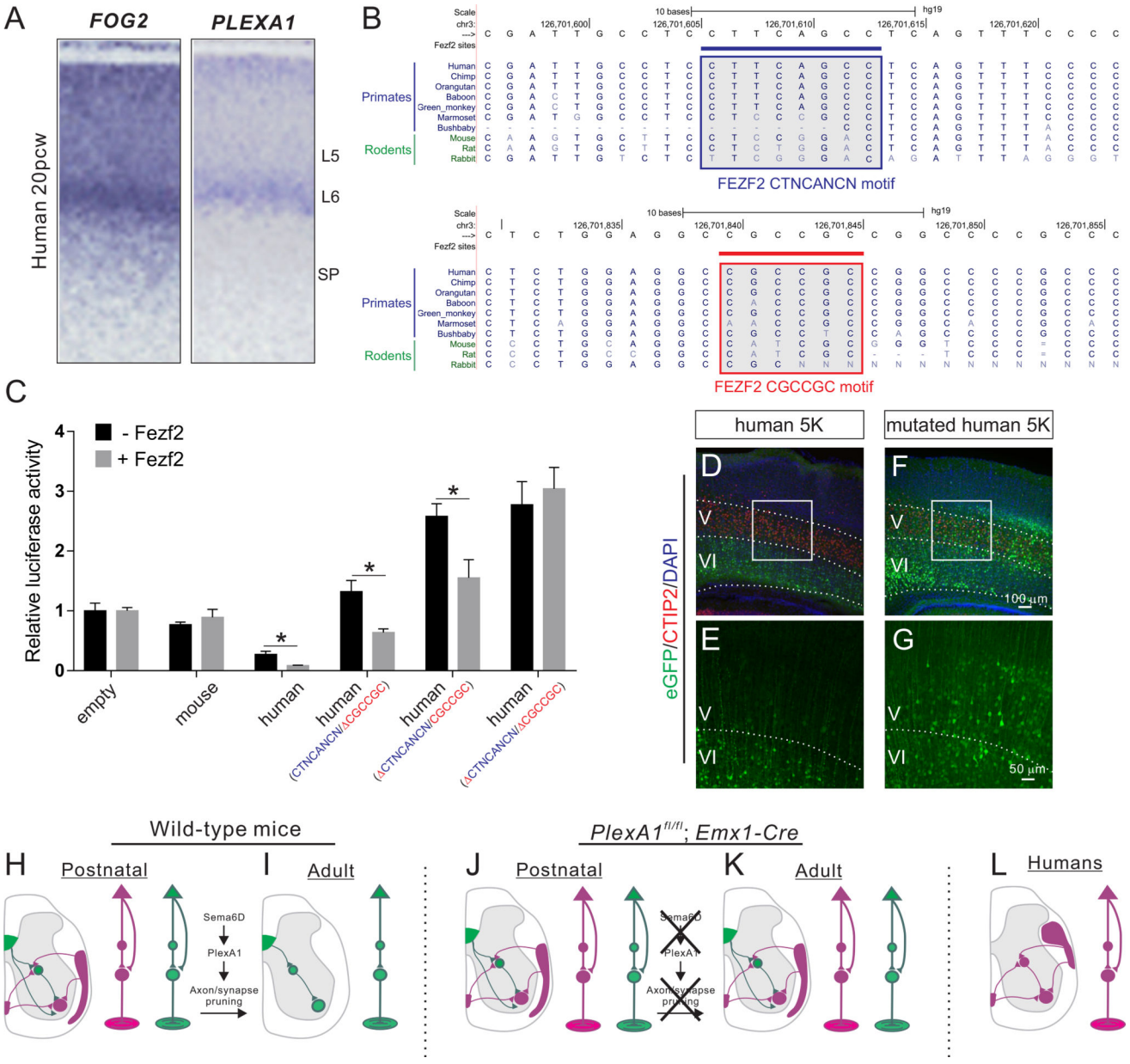

Fig. 4. Expression of *PLEXA1* in layer 5 of the motor cortex in mice and humans, and FEZF2-mediated repression

(**A**) *FOG2* (layer 6 marker) and *PLEXA1* in the human motor cortex at 20 pcw assessed by *in situ* hybridization. (**B**) Sequence conservation of putative *PlexA1 cis*-regulatory elements. Multi-species DNA sequence alignment showing one example of FEZF2 CTNCANCN binding sites (top, blue bar and box) and CGCCGC binding sites (bottom, red bar and box). The motifs are highlighted by gray-filled boxes. (**C**) Luciferase activity of reporter constructs in a 293T cell line (expressing endogenous human *Fezf2*) with or without co-transfection with a human *FEZF2*-expressing vector. Error bars represent the SEM of triplicate experiments. (**D–G**) Analysis of transgenic mice using a 5 Kb region upstream from the first exon of the human *PLEXA1* gene or mutated human FEZF2 binding sequences. (**E–G**) High magnification view of the boxed areas in D and F. (**H–L**) Summary

of the axonal trajectories and CS connectivity within the cervical spinal cord in wild-type and *PlexA1*$^{fl/fl}$*; Emx1-Cre* mice, and in humans.